IET Communications

The Institution of Engineering and Technology WILEY

ORIGINAL RESEARCH PAPER

Research on PDMA system based on complementary sequence and low complexity detection algorithm

Shufeng Li[1] | **Baoxin Su**[1] | **Libiao Jin**[1] | **Yao Sun**[2] | **Zhiping Xia**[3]

[1] The State Key Laboratory of Media Convergence and Communication, School of Information and Communication Engineering, Communication University of China, Beijing, China

[2] James Watt School of Engineering, University of Glasgow, Scotland, UK

[3] Academy of Broadcasting Science, Beijing, China

Correspondence
Shufeng Li, the State Key Laboratory of Media Convergence and Communication, School of Information and Communication Engineering, Communication University of China, Beijing 100024, China.
Email: lishufeng@cuc.edu.cn

Funding information
Central University Basic Research Fund of China, Grant/Award Number: CUC210B032; National Natural Science Foundation of China, Grant/Award Number: 61601414

Abstract

With the intensive deployment of mobile networks and the vigorous development of new multimedia services, video has gradually become the mainstream of cultural consumption. The contradiction between the proliferation of video data services and the scarcity of spectrum resources has brought great challenges to the current network resource allocation. Non-orthogonal multiple access (NOMA) can be used to solve this problem by signal superposition and spectrum multiplexing to improve system access capability. As a new type of joint optimization design of transmitter and receiver side, PDMA has high research value. In this paper, a framework of PDMA video transmission system based on H.264 video compression coding (HVC-PDMA) is proposed. Poly complementary sequence (PCS) spread spectrum coding is performed on the transmission codebook in order to improve the transmission accuracy. Meanwhile, a low complexity serial sphere compensated Max-log MPA (SSCM-MPA) algorithm is proposed to reduce the complexity of the multi-user detection algorithm. Simulation results show that the PCS spread spectrum can improve system throughput and peak signal-to-noise ratio (PSNR) while reducing bit error rate (BER). SSCM-MPA algorithm can greatly reduce the complexity and improve the transmission efficiency.

1 | INTRODUCTION

Non-orthogonal multiple access (NOMA) technology is a key technology of the future cellular mobile communication system [1–4]. It provides services for users under different channel conditions through signal superposition transmission and spectrum multiplexing, improves the access capability and spectrum resource utilization of the system, and effectively meets the connection requirements of hundreds of millions of devices in the network [5]. In contrast to the family of conventional orthogonal multiple access (OMA) schemes, the key distinguishing feature of NOMA is to support a higher number of users than the number of orthogonal resource slots with the aid of non-orthogonal resource allocation. NOMA is considered to be the most promising spectrum access technology for 6G. It allows multiple users to use the same spectrum, so as to improve the spectrum efficiency and reduce the delay, and it can meet the needs of 6G large connection and high frequency spectrum efficiency in the future [6, 7].

Pattern division multiple access (PDMA) is a new NOMA technology with joint optimization design of transmitter and receiver side [8, 9]. PDMA constructs unequal diversity by mapping each user's data to a group of resources with a specific pattern. A group of resources mapped by PDMA can be one or any combination of time, frequency and spatial domain resources [10–12]. At the transmitter side, the signals of multiple users are mapped to the same time, frequency and spatial domain resources for multiplexing transmission while at the receiver side, the serial interference cancellation (SIC) detection algorithm or message passing algorithm (MPA) is used for multi-user detection [12]. Compared with other multiple access technologies, PDMA technology has the advantages of wider application scope and higher flexibility. PDMA can use multi-dimensional domain to design non-orthogonal feature patterns independently or jointly, make full use of multi-dimensional domain processing, and there is no limit on the number of users sharing the same resources.

With the advent of the mobile network era, the dissemination channels of video programs have gradually changed from TV-based to mobile network terminals. Due to the explosive growth of video content, cellular data traffic is growing rapidly, which has brought great pressure on the limited wireless spectrum resources [13]. The combination of NOMA and video transmission can effectively cope with the continuous growth of spectral efficiency and system capacity. Some researches have been carried out on the system analysis of NOMA combined with video transmission [14–17]. Most of these papers focus on the research of video field. In this paper, we focus on the research of bit stream communication transmission.

Considering that video data transmission needs to occupy a large channel capacity, it is easy to cause network jam in the process of transmission [18]. Therefore, data compression is particularly important in solving the problem of large amount of information transmission. H.264 coding is a widely used high-precision video recording, compression and publishing format [19]. Compared with other coding standards, H.264 has higher video quality and lower bit rate. It can enhance the coding efficiency of image, and improve the transmission efficiency of image data in the network [20]. H. 264 is widely used in the fields of network streaming media data, all kinds of HDTV terrestrial broadcasting and satellite television broadcasting [21]. This paper proposes a PDMA video transmission system model based on H.264 video compression coding (HVC-PDMA). It transmits different video data for multiple users through joint multiplexing of single or multiple domains, so as to improve the access capability and spectrum resource utilization.

The interference between users is a common problem in NOMA system. Due to the large amount of video data, the increase of interference between transmission codebooks will directly affect the detection complexity and recovery accuracy. In order to improve the reliability of the system, a design method of multiple input multiple output (MIMO) radar waveform combining direct sequence spread spectrum coding was proposed in [22], which is orthogonal at the transmitter and the receiver side. In [23], a circular superposition spread spectrum scheme for multiple input multiple output (MIMO) underwater acoustic communication was proposed, which forms multiple spread spectrum sequences through cyclic shift and has higher robustness. The binary Golay code spread spectrum of uplink grant free NOMA was studied in [24], the multi carrier signal transmitted by spread spectrum can provide higher power efficiency for equipment. Considering the limited number of binary sequence address codes, and the cross-correlation function is not ideal, in this paper we select poly complete complementary (PCS) as the spread spectrum code to process the transmission signal, so as to improve the reliability of system transmission. Complete complementary sequence is a generalization of Golay complementary codes, which is a set of sequences with ideal correlation sum [25, 26]. As a multi-codebook set in complex field composed of multiple subsequences, the PCS can achieve zero cross-correlation value and reduce the interference among users by using the complementarity between subsequences. Because of its perfect aperiodic correlation, it has been widely used in many fields [27–29].

The choice of multi-user detection algorithm at the receiver side has an important impact on the transmission accuracy of PDMA [30]. The commonly used nonlinear detection algorithms in PDMA are SIC and MPA. However, due to the problem of error propagation in SIC algorithm, the detection performance is not ideal when there are too many transmitted data. MPA detection algorithm has high detection accuracy, so we select MPA for multi-user detection, but at the same time, reducing the complexity of MPA is a major problem. [31] proposed an MPA scheme based on the serial message update strategy of SCMA system, which reduces the complexity by accelerating the convergence speed. According to the AWGN variance, a MPA detection scheme based on sphere decoding was proposed in [32] to dynamically balance the performance and complexity. Due to the huge amount of data information generated during video transmission, it brings great detection complexity and delay. The complexity of these improved MPA detection algorithms is still high, which is not enough to meet the needs of video transmission. From [33] and [34], we can see that outer iterations can be further employed to reduce the computational complexity. However, since this is not the main focus of our work, we skip the detailed discussions on the outer iterations, and more details can be found in [33] and [34]. In order to further reduce the complexity, we comprehensively consider the serial strategy, set the spherical radius and Max-log operation. Considering the above several factors, we propose a serial sphere compensated Max-log MPA (SSCM-MPA) detection algorithm based on the transmission characteristics of PDMA.

The main contributions of this paper are as follows:

- We develop a PDMA-based H.264 video compression (HVC-PDMA) framework for mobile networks. In order to adapt to the multi-order modulation of PDMA, the multivariate conversion of video coding signal to improve the system access capability and spectrum resource utilization.

- Under the framework of HVC-PDMA, we further combine the spread spectrum technology which use PCS to spread spectrum the modulated transmission codebook. Compared with the traditional NOMA transmission mode, PCS spread spectrum processing has obvious advantages in spectrum utilization, throughput and bit error performance (BER).

- A SSCM-MPA low complexity multi-user detection algorithm is proposed. By combining the serial strategy, setting spherical radius and Max-log operation with the MPA receiving algorithm, the complexity of detection algorithm is reduced. Considering the information loss of approximate calculation, information compensation is set to improve the detection accuracy. Meanwhile, the complexity of several receiving algorithms is calculated and compared.

The rest of this paper is organized as follows. Section 2 introduces the HVC-PDMA transmission system model. Section 3 introduces the SSCM-MPA multi-user detection algorithm. In Section 4, the performance of the design scheme is discussed in detail through simulation. Finally, we summarize the whole paper in Section 5.
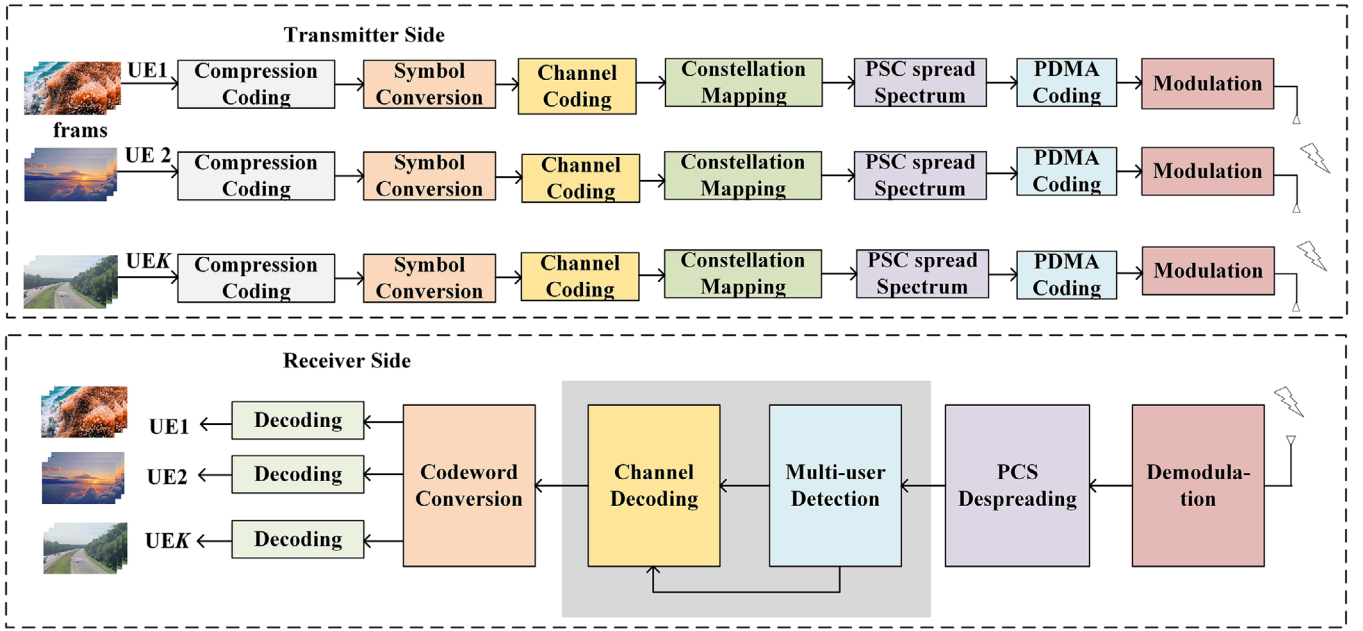
FIGURE 1 HVC-PDMA system model

2 | HVC-PDMA SYSTEM MODEL

Considering the contradiction between the scarcity of wireless spectrum resources and the huge amount of video data transmitted, a HVC-PDMA system model is proposed. As shown in Figure 1, which combines H.264 video coding with PDMA technology to effectively use the same time frequency resources. It greatly improves the link utilization of communication system and saves spectrum resources.

2.1 | Principle of PDMA

PDMA maps transmitted data onto a group of resources according to the patterns to realize disparate transmission diversity order. A PDMA pattern defines the mapping from transmitted data to resource groups which is consist of time resource, frequency resource, spatial resource, or any combination of them. Data of multiple users can be multiplexed onto the same resource group with a different PDMA pattern. In this way, non-orthogonal transmission is realized.

In the uplink PDMA system, the data of K users are mapped to N RBs through different feature patterns $\mathbf{f}_k$. The PDMA pattern matrix is represented by

$$\mathbf{F}_{PDMA}^{[N \times K]} = [f_1, f_2, \dots, f_K]. \tag{1}$$

As shown in Figure 2, the data of six users are mapped to four RBs through different patterns. The PDMA modulation vector $\mathbf{v}_k$ of user k is

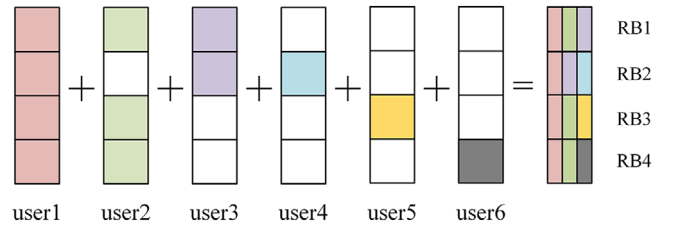$$v_k = f_k x_k, \quad 1 \le k \le K, \tag{2}$$

FIGURE 2 Multi-user mapping of $F_{PDMA}^{[4 \times 6]}$

where $\mathbf{f}_k$ is the binary vector of $N \times 1$ and contains elements "1" and "0" to indicate that the element is mapped to the corresponding RB or not. $\mathbf{x}_k$ is the modulation symbol of user k's data after constellation mapping.

The received signal of base station is given by

$$y = \sum_{k=1}^{K} diag(h_k) v_k + n, \tag{3}$$

where n is the received interference and noise, $\mathbf{h}_k$ is the channel response of the kth user equipment (UE), and $diag(\mathbf{h}_k)$ is the diagonal matrix with element $\mathbf{h}_k$. Equation (3) can be simplified as

$$y = Hx + n, \tag{4}$$

where H is the equivalent channel response matrix of K users multiplexed on N RBs,

$$x = [x_1, x_2, \dots, x_K]^T, \tag{5}$$

$$H = H_{CH} \odot F_{PDMA}^{[N \times K]}, \tag{6}$$

where $H_{CH} = [b_1, b_2, \ldots, b_K]$ is rayleigh channel response matrix. Therefore, Equation (4) can be expressed as

$$
\begin{aligned}
y &= H_{CH} \cdot F_{PDMA}^{[N \times K]} x + n \\
&= [b_1, b_2, \ldots, b_K] \cdot F_{PDMA}^{[N \times K]} [x_1, x_2, \ldots, x_k]^T + n^{[N \times 1]}.
\end{aligned}
\tag{7}
$$

Overload factor is defined as the ratio between the number of UEs and RBs in a resource group. It reflects the multiplexing times of PDMA relative to orthogonal scheme. The overload factor is

$$
\lambda = \frac{K}{N}.
\tag{8}
$$

Taking $N = 4$, $K = 6$ as an example, the $\lambda = 150\%$, which means that PDMA supports 1.5 times user compared with OMA. The PDMA pattern matrix can be expressed as

$$
F_{PDMA}^{[N \times K]} = \begin{bmatrix} 1 & 1 & 1 & 0 & 0 & 0 \\ 1 & 0 & 1 & 1 & 0 & 0 \\ 1 & 1 & 0 & 0 & 1 & 0 \\ 1 & 1 & 0 & 0 & 0 & 1 \end{bmatrix}.
\tag{9}
$$

Substituting the data into Equation (7) we can get

$$
\begin{bmatrix} y_1 \\ y_2 \\ y_3 \\ y_4 \end{bmatrix} = \begin{bmatrix} b_{11} & b_{12} & b_{13} & 0 & 0 & 0 \\ b_{21} & 0 & b_{23} & b_{24} & 0 & 0 \\ b_{31} & b_{32} & 0 & 0 & b_{34} & 0 \\ b_{41} & b_{42} & 0 & 0 & 0 & b_{46} \end{bmatrix} \begin{bmatrix} x_1 \\ x_2 \\ x_3 \\ x_4 \\ x_5 \\ x_6 \end{bmatrix} + \begin{bmatrix} n_1 \\ n_2 \\ n_3 \\ n_4 \end{bmatrix}.
\tag{10}
$$

2.2 | H.264 encoding

H.264 coding has the advantages of high fault tolerance and high image quality. Therefore, H.264 coding can be used in both long-distance and short-distance network signal transmission. H.264 has become the video compression standard of HDTV or IPTV in many countries [35]. Because of the combination of multiple reference frame mode prediction, multi-mode motion estimation (ME), integer transform and quantization, loop filtering and advanced entropy coding technology, the coding efficiency has been greatly improved.

H. 264 is a mixed coding mode, which is mainly divided into prediction coding, transform coding and entropy coding. Figure 3 is the functional block diagram of H.264 encoder. Spatial and temporal redundant components are eliminated by inter and intra prediction, and frequency domain redundant components are eliminated by transform and quantization coding [36]. H. 264 video coding divides image frames into I-frames, P-frames and B-frames according to different reference data sources. In H.264, images are organized by sequences, a sequence is a data stream after image coding, starting with

I-frame and ending with the next I-frame. Considering the backward reference characteristics of B-frames will bring coding delay, B-frames are not considered in real-time communication and video sequence simulation in this paper.

Intra compression is a method to generate I-frames. First, based on the principle of rate distortion optimization, selects the best intra prediction mode to obtain the predicted value P, and then subtracts the current actual value and P to obtain the residual block D_n, after transformation(T), quantization(Q) and other processes, the transformation coefficient X is obtained. On the one hand, X encodes the code stream through reordering and entropy coding, reconstructs the prediction residual image D_n' through operations such as inverse quantization and inverse transformation, inverse transformation and other operations, and then adds it with P to get the reconstructed frame uF_n'. Finally, it is sent to the filter for smoothing, and the reconstructed frame image F_n' similar to the original image can be obtained and stored for the reference of the later image coding.

Inter frame compression is a method to generate P-frames, and the macroblocks in the previously encoded frames should be selected as the reference for inter frame coding. First, ME is performed on the image. ME is to find the motion trajectory of similar blocks from adjacent frames to obtain their motion vectors, and express the original value of the image by using the sum of motion vectors, residual data and predicted value [37].

After motion compensation (MC) prediction or intra prediction, the residual data block needs to be reshaped and transformed, and the discrete cosine transform is changed into an approximate integer transform, which can reduce the types of coefficients and reduce the amount of computation. Part of the information after shaping will be integrated into the quantization process. First, the input block B is transformed to obtain the unscaled coefficient W,

$$
W = CBC^T,
\tag{11}
$$

where C is the transformation matrix,

$$
C = \begin{bmatrix} a & a & a & a \\ b & c & -c & -b \\ a & -a & -a & a \\ c & -b & b & -c \end{bmatrix},
\tag{12}
$$

where $a = 1/2$, $b = \sqrt{1/2} \cos(\pi/8)$, $c = \sqrt{1/2} \cos(3\pi/8)$.

For each coefficient W_{ij} to complete quantization and scaling at the same time, where W_{ij} is the element of ith row and j^{th} column of W, the quantization matrix is formulated as

$$
Z_{ij} = round\left(W_{ij} \frac{MF + f}{2^{qbits}} \right).
\tag{13}
$$

It is known that

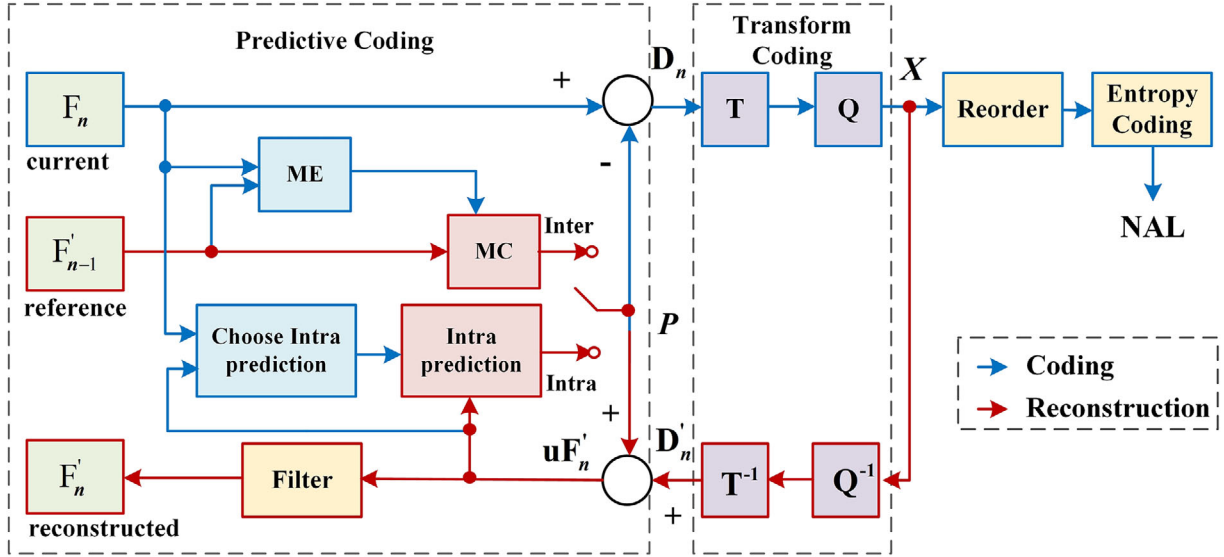$$
qbits = 15 + floor\left(\frac{QP}{6}\right),
\tag{14}
$$

FIGURE 3 H.264 encoding block diagram

$$MF = \frac{PF}{Q_{\text{step}}} 2^{qbits}, \qquad (15)$$

$$f = \begin{cases} \dfrac{2^{qbits}}{3} & , \text{intraframe} \\ \dfrac{2^{qbits}}{6} & , \text{interframe} \end{cases}, \qquad (16)$$

where QP is the quantization parameter, Q_{step} is the quantization step and PF is the backward scaling factor. In order to simplify the operation, the product factor $\dfrac{PF}{Q_{step}}$ can be realized by shifting the factor MF to the right to avoid division.

In order to correspond to the modulation order M of PDMA, every $\log_2 M$-bit codeword of the transmitted codebook after compression coding is regarded as a binary array for M-ary conversion. When the number of binary symbols cannot be divided by M, the zeros will be filled later. The transmission signal x_k can be obtained.

2.3 | PCS spreading spectrum

Complete complementary sequence is a set of complementary sequences with ideal auto-correlation and cross-correlation. Different from the traditional single codebook spread spectrum sequence, it is a joint design scheme of multiple codebooks. Based on the principle of correlation complementarity between multiple codebook subsequences, the codebook sequence with zero cross-correlation value is obtained to eliminate the interference between users. Due to the limited number of codebook of the binary sequence and the unsatisfactory cross-correlation function, thus we choose PCS as the spread spectrum sequence. Figure 4 is the structure diagram of PCS model.

The set of complementary sequences with length L can be expressed as $\{(A_1, B_1), (A_2, B_2), \dots, (A_K, B_K)\}$, where (A_k, B_k)
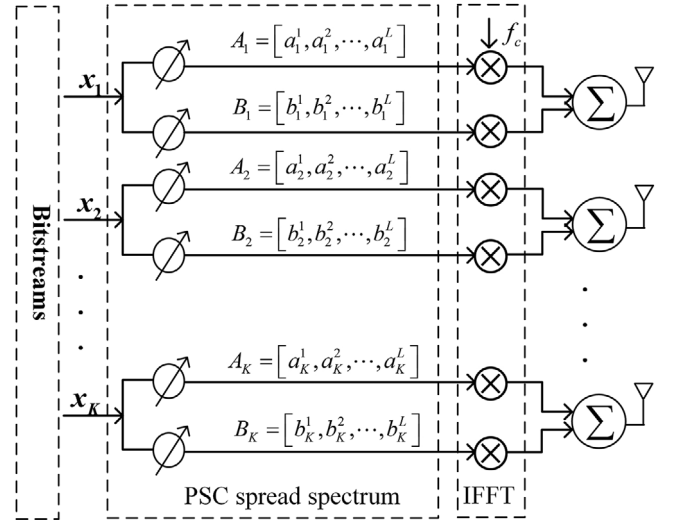

FIGURE 4 PCS model structure diagram

forms a pair of complementary sequences and satisfies complete orthogonality. Take the four phase sequence as an example,

$$\begin{cases} A_k = \left(a_k^0, a_k^1, \dots, a_k^{L-1}\right) \\ B_k = \left(b_k^0, b_k^1, \dots, b_k^{L-1}\right) \end{cases}, \qquad (17)$$

where $a_k^l, b_k^l \in (-1, 1, j, -j)$. Their aperiodic auto-correlation function $\varphi(\tau)$ satisfies

$$\varphi_A(\tau) + \varphi_B(\tau) = \begin{cases} 2L & \tau = 0 \\ 0 & \tau \neq 0 \end{cases}. \qquad (18)$$

Table 1 shows several corresponding sequences.

TABLE 1 Simulation parameter settings

Given sequence	$A_k = (a_k^0, a_k^1, \ldots, a_k^{L-1})$
Reverse sequence	$\tilde{A}_k = (a_k^{L-1}, a_k^{L-2}, \ldots, a_k^0)$
Negative sequence	$\hat{A}_k = (-a_k^0, -a_k^1, \ldots, -a_k^{L-1})$
Even bit negation sequence	$\overset{*}{A}_k = (a_k^0, -a_k^1, \ldots, (-1)^{L-1} d_k^{L-1})$

FIGURE 5 MPA factor graph of $F_{PDMA}^{[4 \times 6]}$

According to the properties of complementary sequences, $(A_k, \tilde{B}_k), (\tilde{A}_k, \tilde{B}_k), (A_k, \hat{B}_k), (\hat{A}_k, \hat{B}_k), (\overset{*}{A}_k, \overset{*}{B}_k)$ etc. also constitute complementary sequences.

A_k and B_k encode the user data in turn, and the kth spread spectrum sequence can be expressed as

$$c_k(t) = A_k(t) + B_k(t - \tau_0)$$

$$= \sum_{l=0}^{L-1} \left[d_k^l rect\left(\frac{t - (l+1)T_c}{LT_c}\right) + \right.$$

$$\left. b_k^l rect\left(\frac{t - (l+1)T_c - \tau_0}{LT_c}\right) \right], \quad (19)$$

where T_c is the chip period, τ_0 is the transmission time delay, and $rect$ is the rectangular window function.

$$rect(t) = \begin{cases} 1 & 0 \le t \le T_c \\ 0 & else \end{cases}. \quad (20)$$

Let $\mathbf{x}_k$ denote the transmission signal of the kth user with length D after compression coding, $\mathbf{x}_k = [\mathbf{x}_k^1, \mathbf{x}_k^2, \ldots, \mathbf{x}_k^D]$. The transmission signal x is

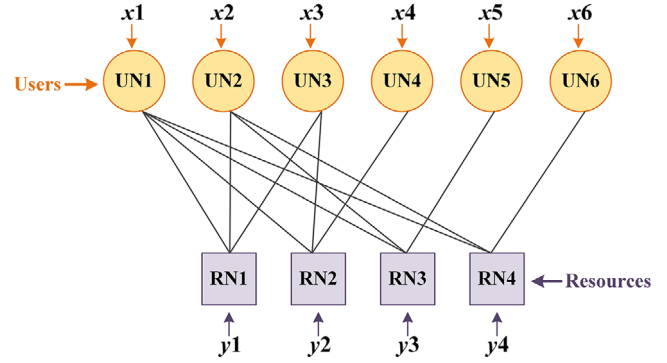$$x = \begin{bmatrix} \mathbf{x}_1^1 & \mathbf{x}_1^2 & \cdots & \mathbf{x}_1^D \\ \mathbf{x}_2^1 & \mathbf{x}_2^2 & \cdots & \mathbf{x}_2^D \\ \cdots & \cdots & \cdots & \cdots \\ \mathbf{x}_K^1 & \mathbf{x}_K^2 & \cdots & \mathbf{x}_K^D \end{bmatrix}. \quad (21)$$

The dth group of transmission signals $\mathbf{x}^d = [\mathbf{x}_1^d, \mathbf{x}_2^d, \ldots, \mathbf{x}_K^d]^T$ after PCS spread spectrum is formulated as

$$s_d(k, :)(t) = \mathbf{x}_k^d A_k(t) + \mathbf{x}_k^d B_k(t - \tau_0)$$

$$= \mathbf{x}_k^d \sum_{l=0}^{L-1} \left[d_k^l rect\left(\frac{t - (l+1)T_c}{LT_c}\right) + \right.$$

$$\left. b_k^l rect\left(\frac{t - (l+1)T_c - \tau_0}{LT_c}\right) \right]. \quad (22)$$

The received signal can be specifically expressed as

$$y_d = H_{CH} \cdot F_{PDMA}^{[N \times K]} s_d + n^{[N \times L]}. \quad (23)$$

The received signal y with dimension $[N \times D]$ can be obtained by despreading each group of signals, and then the corresponding transmission signal can be obtained by multi-user detection algorithm at the receiver side.

3 | SSCM-MPA MULTI-USER DETECTION ALGORITHM

The MPA detection algorithm has high detection accuracy and is more suitable for large data signal transmission detection such as video data, while its complexity will increase exponentially with the increase of the modulation order. In order to reduce the complexity of MPA, we propose a SSCM-MPA to reduce the number of iterations required for convergence. The serial strategy can transfer the updated information of resource nodes (RNs) to user nodes (UNs) in time, and accelerate the convergence speed of node information update. Setting the spherical radius can reduce the constellation points involved in the iteration and the computational complexity [35]. Max-log converts multiplication to addition, which can also reduce the complexity of the algorithm. However, due to several approximate operations, it is necessary to compensate the missing part of iterative information to improve the detection accuracy.

MPA detection is accomplished by message passing and iterative updating between RNs and UNs in factor graph, as shown in Figure 5. The implementation process mainly includes the following three stages:

Stage 1: The transition probability between each UN and its RN is initialized, and the probability of each user's codeword superimposed on its connected resource block is equal.

Stage 2: All RNs update the message from all RNs to UN with the information passed by UNs as prior information.

Stage 3: All UNs update the messages passed by the synthetic RN, and update the message from all UNs to RN in factor graph.

$\varphi(y_n | x_n)$ is the probability density function which can be expressed as

$$\varphi(y_n | x_n) = \frac{1}{\sqrt{2\pi\sigma^2}} \exp\left(\frac{-1}{2\sigma^2} \left\| y_n - \sum_{m \in \upsilon(n)} h_{n,m} x_{n,m} \right\|^2\right), \quad (24)$$

where x_n is defined as the combination of codewords that may be sent by all users connected on resource block n.

The message passing between nodes is given by

$$M^t_{r_n \to u_k}(x_k) = \sum_{\sim\{x_k\}} \left\{ \varphi(y_n|x_n) \prod_{p \in \upsilon(n)\backslash k} M^{t-1}_{u_p \to r_n}(x_p) \right\}, \quad (25)$$

$$M^t_{u_k \to r_n}(x_k) = \prod_{m \in U(k)\backslash n} M^t_{r_m \to u_k}(x_k), \quad (26)$$

where t is the number of iterations, σ is the noise variance, $\upsilon(n)$ and $U(k)$ represent the non-zero position set of the nth row and the kth column of the pattern matrix F, respectively.

For the external information from UN to RN can only be transferred in the next iteration, the correction of the external information is relatively slow, and the convergence speed of the detector iteration is also limited. The use of the serial structure for message transmission can accelerate the convergence. In this case, Equation (25) can be rewritten as

$$M^t_{r_n \to u_k}(x_k) = \sum_{\sim\{x_k\}} \left\{ \varphi(y_n|x_n)\xi(p) \right\}, \quad (27)$$

where

$$\xi(p) = \prod_{p>k, p\in\upsilon(n)\backslash k} M^{t-1}_{u_p \to r_n}(x_p) \prod_{p<k, p\in\upsilon(n)\backslash k} M^t_{u_p \to r_n}(x_p). \quad (28)$$

According to the spherical decoding theory, the closer the Euclidean distance of the composite constellation point is to the received signal point, the more likely it is to decode correctly [31]. In order to further reduce the complexity, we set a sphere radius R to reduce the number of user codewords participating in the iteration.

$$\eta = \left\| y_n - \sum_{m\in\upsilon(n)} h_{n,m}x_{n,m} \right\| \leq R = \alpha\sigma, \quad (29)$$

where η is the Euclidean distance between the composite constellation point and the received signal, and α is a real number greater than 0. According to the normal distribution, the probability of correct decoding can reach 95.4% at $R = 2\sigma$, which can meet the normal demand.

At this time, the message passing of serial sphere MPA detection algorithm is given by

$$M^t_{r_n \to u_k}(x_k) = \sum_{\eta \leq R} \left\{ \varphi(y_n|x_n) \cdot \xi(p) \right\}. \quad (30)$$

Max-log calculation can transform complex exponential calculations into simple calculations, greatly reducing the amount

of detector calculations and data storage. The main idea of Max-log detection algorithm is

$$\log\left(\sum_{i=1}^{N} \exp(f_i) \right) \approx \max\{f_1, f_2, ..., f_N\}, \quad (31)$$

The message passing of serial Max-log MPA (SM-MPA) detection algorithm is formulated as

$$\log\left(M^t_{r_n \to u_k}(x_k)\right) = \log\left\{ \max\left[\varphi(y_n|x_n)\right] \right\} + \log\left[\xi(p)\right]. \quad (32)$$

Then we can get the message passing of serial sphere Max-log MPA (SSM-MPA) detection algorithm,

$$\log\left(M^t_{r_n \to u_k}(x_k)\right) = \log\left\{ \max_{\eta\leq R}\left[\varphi(y_n|x_n)\right] \right\} + \log\left[\xi(p)\right]. \quad (33)$$

As known

$$\log\left(\sum_{i=1}^{N} \exp(a_i) \right) > \max\{a_1, a_2, ..., a_N\}. \quad (34)$$

Obviously, using Max-log operation will cause partial information loss. Therefore, considering the information loss and accuracy loss caused by approximate calculation, this paper introduces signal compensation to improve the accuracy of approximate calculation and provide more reliable information for the next iteration process. In [38], the Jacobian algorithm is proposed to simplify the logarithm summation,

$$\ln\left(e^\alpha + e^\beta\right) = \max(\alpha, \beta) + \ln\left(1 + e^{-|\alpha-\beta|}\right). \quad (35)$$

Inspired by this, we can get $e^{-|\alpha-\beta|} \in (0, 1]$,

$$\ln\left(1 + e^{-|\alpha-\beta|}\right) \in (0, 0.69]. \quad (36)$$

Adding the maximum compensation of 0.69 to the RN update data, Equation (33) can be expressed as

$$\log\left(M^t_{r_n \to u_k}(x_k)\right) = \log\left\{ \max_{\eta\leq R}\left[\varphi(y_n|x_n)\right] \right\} + 0.69 + \log\left[\xi(p)\right]. \quad (37)$$

This not only retains the advantage of lower complexity, but also compensates for the message value obtained by the RNs during each iteration, which is closer to the true value, providing more reliable information for the subsequent iteration process and improving detection accuracy. The flow of SSCM-MPA multi-user detection algorithm is shown in Algorithm 1.

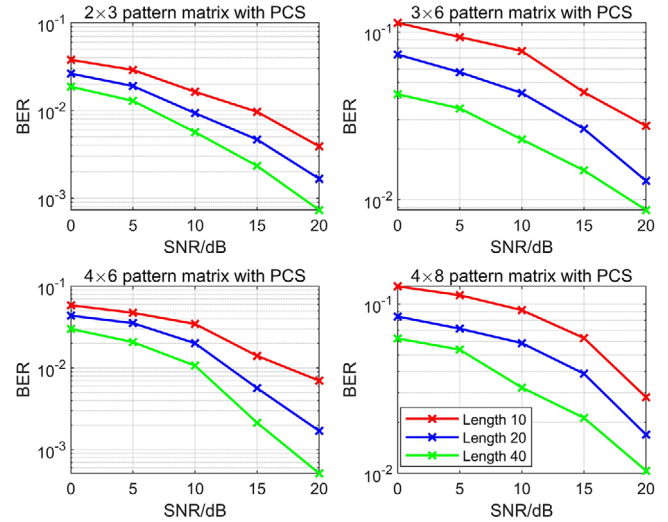**ALGORITHM 1** SSCM-MPA Multi-user Detection Algorithm

1:    **Input**: $y, \sigma, H, F, N, K, M, t_{\max}$

2:    **Initialization**: let $v = []$.

3:    **for** $m=1{:}M$ **do**

4:       $v(:,:,m) = F$

5:       **for all** $n, k \in U(k)$ **do**

6:          $v(n, k, m) = \frac{1}{M}$

7:       **end for**

8:    **end for**

9:    we can get $M^0_{r_n \to u_k}(x_k) = \frac{1}{M}$ and $M^0_{u_k \to r_n}(x_k) = \frac{1}{M}$.

10:    **Iteration**:

11:    **for** t $= 1{:}t_{\max}$ **do**

12:       **Calculate contingent probability**:

13:       **for all** $n, k \in V(n)$ **do**

14:          **for** $m=1{:}M$ **do**

15:             calculate η via Equation (29).

16:          **end for**

17:       **end for**

18:       **Information update**:

19:       let $R = 2\sigma$

20:       **for all** $n, k \in V(n)$ **do**

21:          **for** $m=1{:}M$ **do**

22:             **if** abs$(\eta) \le R$ **then**

23:                update $M^t_{r_n \to u_k}(x_k)$ via Equation (37).

24:             **end if**

25:          **end for**

26:       **end for**

27:    **end for** (Iteration)

28:    **Output**: get the detection information, and calculate BER, PSNR or other performance.

FIGURE 6   BER of PCS spread spectrum with different pattern matrices

TABLE 2   Simulation parameter settings

Simulation parameters	Numerical value
Channel model	Rayleigh channel
Number of RB (N)	4
Number of UE (K)	6
Overload rate	150%
Modulation	QPSK
Modulation order (M)	4
Spherical radius (R)	2σ
Iterations (t)	10
QP	20

4 | SIMULATION RESULTS DISCUSSION

In this section, we have carried on the simulation analysis to the above research point. First, the performance of the HVC-PDMA system with joint PCS spread spectrum is analyzed. Then the complexity of the SSCM-MPA detection algorithm is analyzed.

Before the simulation analysis, the BER performance of PCS spread spectrum with PDMA pattern matrices in different dimensions is compared. We selected the PDMA pattern matrix with dimensions of 2×3, 3×6, 4×6 and 4×8, respectively. As mentioned above, PDMA transmits the signals of multiple users through pattern mapping, the greater the overload rate, the more users the system will carry, but the signal interference between users will increase accordingly, which will affect the bit error performance of the transmission signal to a certain extent. Through simulation, it can be seen from Figure 6 that the BER trend of pattern matrix with the same overload rate is similar, and the BER of 150% overload rate is slightly better than

200%. Therefore, combined with the transmission capacity and comprehensive consideration, we select 4×6 pattern matrix for simulation. The parameter values involved in the simulation are shown in Table 2.

4.1 | Performance analysis of HVC-PDMA system based on PCS spread spectrum technology

In Figure 7, the impact of PCS spreading sequences of different lengths on the accuracy of the HVC-PDMA transmission system is compared. It can be seen from the figure that the BER performance of PCS spread spectrum is better compared with no spread spectrum, and the BER decreases as the length of the PCS spread spectrum sequence increases. When the length of PCS increases from 40 to 80 or even 160, the BER improvement effect is not obvious, but the complexity will be greatly improved. Therefore, it is more appropriate when the length of PCS is 40. This is because the spread spectrum sequence can expand the signal bandwidth. With the same signal-to-noise ratio (SNR), as the spread spectrum sequence
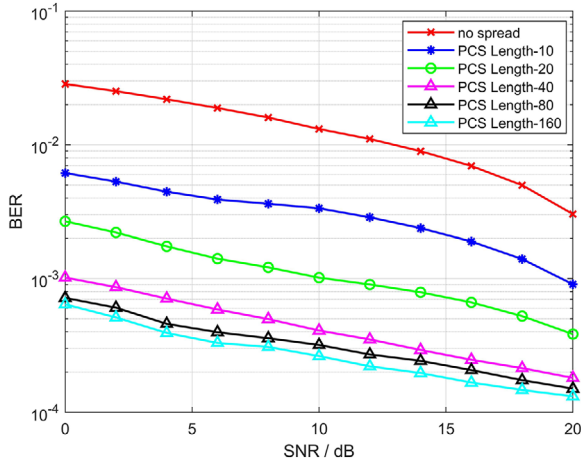
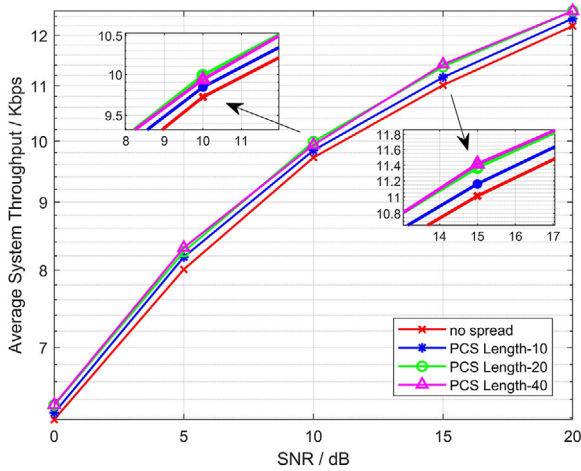**FIGURE 7** BER of video coding under PCS spread spectrum

FIGURE 9 BER of the detection algorithms

FIGURE 8 Throughput of video coding under PCS spread spectrum

TABLE 3 Comparison of complexity

	Algorithms	Number
Adders	MPA	$Dt_{\max}Nd_f(d_f m^{d_f-1} + m^{d_f}d_f)$
	SM-MPA [31]	$Dt_{\max}N\{d_f[m^{d_f-1}(2d_f-1)+2m]+d_f\}$
	SSM-MPA [32]	$Dt_{\max}Nd_f[d_f m^{d_f-1} + (m^{d_f-1}\sum q+1)]$
	SSCM-MPA	$Dt_{\max}Nd_f[d_f(m^{d_f-1}+1)+(m^{d_f-1}\sum q+1)]$
Multipliers	MPA	$Dt_{\max}Nd_f((2d_f+1)m^{d_f-1}+m^{d_f-1})$
	SM-MPA [31]	$Dt_{\max}Nd_f(d_f+1)m^{d_f-1}$
	SSM-MPA [32]	$Dt_{\max}Nd_f[m^{d_f-1}(d_f-1)+m(\sum q+1)]$
	SSCM-MPA	$Dt_{\max}Nd_f[m^{d_f-1}(d_f-1)+m(\sum q+1)]$

increases, the anti-interference performance is also enhanced. Therefore, the combination of PCS as extended codebook and PDMA communication technology can greatly optimize the transmission performance.

Figure 8 compares the average throughput of the HVC-PDMA with PCS spread spectrum sequences. As can be seen from the figure, with the increase of SNR, the throughput increases gradually. PCS spread spectrum can improve the system throughput, but as the length of the spread spectrum sequence continues to increase, the throughput does not increase significantly. This is because the spreading sequence length has an optimal value range, reaching the capacity limit, beyond which the improvement of throughput performance is no longer obvious.

4.2 | Performance analysis of SSCM-MPA multi-user detection algorithm

In Figure 9, the BER performance of detection algorithms under different SNR is compared. As can be seen from the
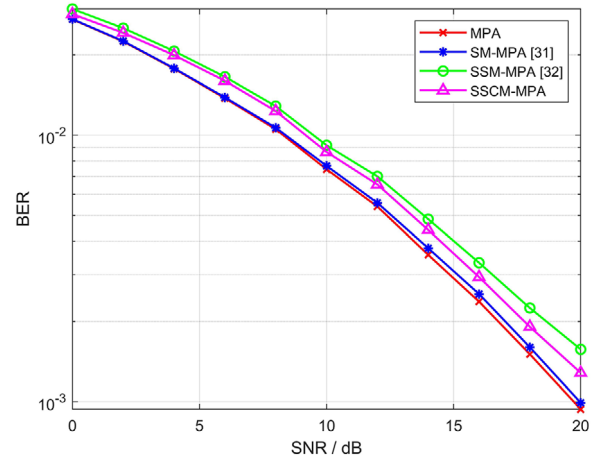
figure, compared with the MPA algorithm, the loss of the BER performance of SM-MPA [31] is not obvious while that of SSM-MPA and SSCM-MPA is more obvious. When the BER is 10^{-2}, the losses of SSM-MPA [32] and SSCM-MPA are nearly 1.46 dB and 0.82 dB, respectively, compared with MPA. Through the calculation of the data, we can see that after information compensation, compared with SSM-MPA, SSCM-MPA can obtain a gain of about 0.64 dB.

The complexity of the detection algorithms is compared in Table 3 and Figure 10, where $t_{\max}$ is the maximum number of iterations, d_f is the number of superimposed users, and q is the constellation point in the range of R. As can be seen from Figure 10, SSCM-MPA has the lowest complexity compared with other algorithms. The multiplication complexity of SSCM-MPA is 62.67% and 33.33% lower than that of MPA and SM-MPA, respectively. Combined with the analysis of BER performance in Figure 9, SSCM-MPA algorithm reduces the number of iterations and greatly reduces the complexity at the cost of losing part of BER, so this scheme is feasible.

Figure 11 compares the convergence performance of different iterations when SNR is 5 dB and 10 dB, respectively. We can see that with the increase of the number of iterations, BER tends to be stable and basically converges in the fourth iteration. And the larger the SNR is, the smaller the BER. This is because with
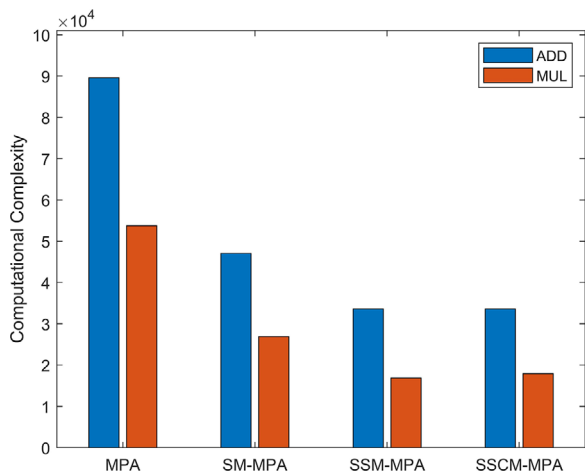
FIGURE 10 Algorithm complexity comparison

FIGURE 12 PSNR of PCS spread spectrum signal detected by SSCM-MPA
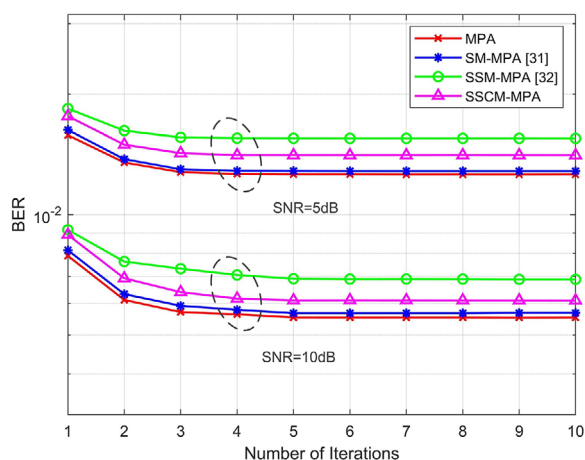

FIGURE 11 Comparison of convergence behavior

the increase of SNR, more effective information is transmitted, the transmission reliability is enhanced, so the BER is smaller.

Figure 12 compares the peak signal-to-noise ratio (PSNR) performance of the PCS spreading sequence combined with the SSCM-MPA detection algorithm in the framework of HVC-PDMA system model. The PSNR increases as the length of the PCS sequence increases. Therefore, we can see that the combined use of PCS spread spectrum and SSCM-MPA detection can reduce image distortion and improve the overall transmission quality of the system.

5 | CONCLUSION

In this paper, a HVC-PDMA video transmission system model is presented. We combine video coding with PDMA transmission technology, and mainly study PCS spread spectrum transmission and SSCM-MPA low complexity detection algorithm. First, we combined the PDMA transmission characteristics and used PCS as the spreading sequence to compare the impact of spreading technology on BER and throughput with
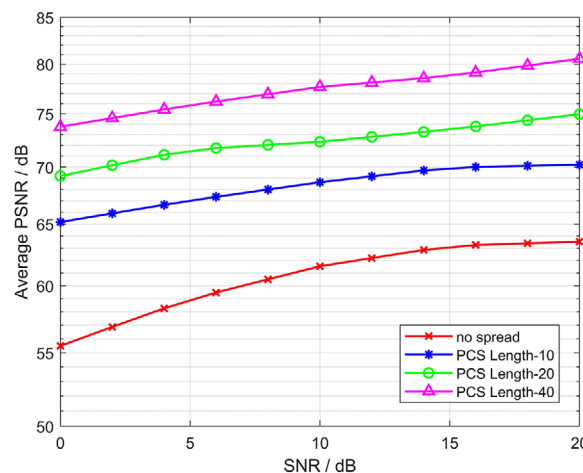
the HVC-PDMA system model. Meanwhile, considering the high complexity of the receiving algorithm when transmitting a large amount of data, we propose a SSCM-MPA multi-user detection algorithm, which combines the serial strategy, sphere detection and Max-log operation to reduce the number of iterations and computational complexity of MPA. In order to reduce the loss of accuracy, information compensation is carried out based on Jacobian algorithm. Simulation results show that PCS spread spectrum transmission can significantly reduce BER and improve part of the throughput. Compared with MPA and SM-MPA, SSCM-MPA can greatly reduce the complexity at the cost of losing part of BER. And as the SNR increases, the system PSNR will also increase since the length of the PCS sequence increases.

DATA AVAILABILITY STATEMENT
Data sharing not applicable to this article as no datasets were generated or analysed during the current study.

CONFLICT OF INTEREST
The authors have declared no conflict of interest.

ORCID
Shufeng Li https://orcid.org/0000-0002-4837-1412

REFERENCES
1. Dai, L., Wang, B., Ding, Z., Wang, Z., Chen, S., Hanzo, L.: A survey of non-orthogonal multiple access for 5G. IEEE Commun. Surv. Tut. 20(3), 2294–2323 (2018)
2. Chen, Y., Bayesteh, A., Wu, Y., et al.: Toward the standardization of nonorthogonal multiple access for next generation wireless networks. IEEE Commun. Mag. 56(3), 19–27 (2018)

3. Yan, L., Yongzhao, L., Yunfei, C., Yinghui, Y., Hailin, Z.: Performance analysis of cooperative NOMA with a shared AF relay. IET Commun. 12(19), 2438–2447 (2018)

4. Sun, Y., Qin, S., Feng, G., Zhang, L., Imran, M.: Service provisioning framework for RAN slicing: User admissibility, slice association and bandwidth allocation. IEEE Trans. Mobile Comput. 20(12), 3409–3422 (2020).

5. Yan, L., Yongzhao, L., Yunfei, C., Yinghui, Y., Hailin, Z.: Performance analysis of cooperative NOMA with a shared AF relay. IET Commun. 12(19), 2438–2447 (2018)

6. Mokdad, A., Azmi, P., Mokari, N.: Radio resource allocation for heterogeneous traffic in GFDM-NOMA heterogeneous cellular networks. IET Commun. 10(12), 1444–1455 (2016). https://doi.org/10.1049/iet-com.2016.0011

7. Sun, Y., Zhang, L., Feng, G., Yang, B., Cao, B., Imran, M.A.: Blockchain-Enabled Wireless Internet of Things: Performance Analysis and Optimal Communication Node Deployment. IEEE Internet of Things J. 6(3), 5791–5802 (2019).

8. Dai, X., et al.: Successive interference cancelation amenable multiple-access (SAMA) for future wireless communications. In: Proceedings of IEEE International Conference on Circuits and Systems, pp. 222–226. IEEE, Piscataway (2014)

9. Jiang, Y., Li, P., Ding, Z., Zheng, F., Ma, M., You, X.: Joint transmitter and receiver design for pattern division multiple access. IEEE Trans. Mob. Comput. 18(4), 885–895 (2019)

10. Wanwei, T., Shaoli, K., Bin, R., Xinwei, Y., Xiurong, Z.: Uplink pattern division multiple access in 5G systems. IET Commun. 12(9), 1029–1034 (2018)

11. Dai, X., Zhang, Z., et al.: Pattern division multiple access (PDMA): A new multiple access technology for 5G. IEEE Wire. Commun. 25(2), 54–60 (2018)

12. Chen, S., Ren, B., Gao, Q., Kang, S., Sun, S., Niu, K.: Pattern division multiple access a novel nonorthogonal multiple access for fifth-generation radio networks. IEEE Trans. Veh. Technol. 66(4), 3185–3196 (2017)

13. Nightingale, J., Salva-Garcia, P., Calero, J., Wang, Q.: 5G-QoE: QoE modelling for Ultra-HD video streaming in 5G networks. IEEE Trans. Broadcast. 64(2), 621–634 (2018)

14. Yang, L., Chen, J., Ni, Q., Shi, J., Xue, X.: NOMA-enabled cooperative unicast–multicast: Design and outage analysis. IEEE Trans. Wireless Commun. 16(12), 7870–7889 (2017)

15. Zhang, M., Lu, H., Wu, F., Chen, C.: NOMA-based scalable video multicast in mobile networks with statistical channels. IEEE Trans. Mob. Comput. 20(6), 2238–2253 (2021)

16. Wu, J., Tan, B., Wu, J., Wang, M.: Video multicast: Integrating scalability of soft video delivery systems into NOMA. IEEE Wireless Commun. Lett. 8(6), 1722–1726 (2019)

17. Sun, Y., et al.: Efficient handover mechanism for radio access network slicing by exploiting distributed learning. IEEE Trans. Netw. Serv. Manage. 17(4), 2620–2633 (2020)

18. Pratap, S., Apte, Shaila, D.: Quality assessment framework for video contextualisation of personal videos. IET Image Proc. 14(3), 545–551 (2020)

19. Tang, Q., Nasiopoulos, P., Ward, R.: Compensation of requantization and interpolation errors in MPEG-2 to H.264 transcoding. IEEE Trans. Circuits Syst. Video Technol. 18(3), 314–325 (2008)

20. Im, S.K., Pearmain, A.J.: Error resilient video coding with priority data classification using H.264 flexible macroblock ordering. IET Image Proc. 1(2), 197–204 (2007)

21. Naziha, K., Atef, M., Fahmi, K., Nouri, M.: Secure chaotic dual encryption scheme for H.264/AVC video conferencing protection. IET Image Proc. 12(1), 42–52 (2018)

22. Cheng, S., Wang, W., Shao, H.: Spread Spectrum-Coded OFDM Chirp Waveform Diversity Design. IEEE Sens. J. 15(10), 5694–5700 (2015)

23. Qin, X., Qu, F., Zheng, Y.: Circular superposition spread-spectrum transmission for multiple-input multiple-output underwater acoustic communications. IEEE Commun. Lett. 23(8), 1385–1388 (2019)

24. Yu, N.: Binary Golay spreading sequences and Reed-Muller codes for uplink grant-free NOMA. IEEE Trans. Commun. 69(1), 276–290 (2021)

25. Golay, M.: Complementary series. IRE Trans. Inf. Theory 7(2), 82–87 (1961)

26. Turyn, R.: Ambiguity functions of complementary sequences (Corresp.). IEEE Trans. Inf. Theory 9(1), 46–47 (1963)

27. Xiaoyu, C., Guanmin, L., Huanchang, L.: Two constructions of zero correlation zone aperiodic complementary sequence sets. IET Commun. 14(4), 556–560 (2020)

28. Massimiliano, Z., Luigi, C., Anna, R., Vajna, K., Zsolt, M.: Dickson charge pump using integrated inductors in complementary metal–oxide semiconductor technology. IET Power Electron. 9(3), 553–558 (2016)

29. Wang, F., Pang, C., Wu, H., Li, Y., Wang, X.: Designing constant modulus complete complementary sequence with high Doppler tolerance for simultaneous polarimetric radar. IEEE Signal Process Lett. 26(12), 1837–1841 (2019)

30. Higuchi, K., Benjebbour, A.: Non-orthogonal multiple access (NOMA) with successive interference cancellation for future radio access. IEEE Trans. Commun. 98(3), 403–414 (2015)

31. Du, Y., Dong, B., Chen, Z., Fang, J., Yang, L.: Shuffled multiuser detection schemes for uplink sparse code multiple access systems. IEEE Commun. Lett. 20(6), 1231–1234 (2016)

32. Yang, L., Ma, X., Siu, Y.: Low complexity MPA detector based on sphere decoding for SCMA. IEEE Commun. Lett. 21(8), 1855–1858 (2017)

33. Dai, J., Niu, K., Lin, J.: Iterative Gaussian-approximated message passing receiver for MIMO-SCMA system. in IEEE J. Sel. Top. Signal Process. 13(3), 753–765 (2019)

34. Chen, L., Hu, B., Xu, G., Chen, S.: Energy-efficient power allocation and splitting for mmWave beamspace MIMO-NOMA with SWIPT. IEEE Sens. J. 21(14), 16381–16394 (2021)

35. McDonagh, P., Pande, A., Murphy, L., Mohapatra, P.: Toward deployable methods for assessment of quality for scalable IPTV services. IEEE Trans. Broadcast. 59(2), 223–237 (2013)

36. Naziha, K., Atef, M., Fahmi, K., Nouri, M.: Secure chaotic dual encryption scheme for H.264/AVC video conferencing protection. IET Image Proc. 12(1), 42–52 (2018)

37. Gao, Y., Wu, Y., Chen, Y.: H.264/advanced video coding (AVC) backward-compatible bit-depth scalable coding. IEEE Trans. Circuits Syst. Video Technol. 19(4), 500–510 (2009)

38. Chen, J., Zhang, Z., He, S., Hu, J., Sobelman, G.: Sparse code multiple access decoding based on a Monte Carlo Markov chain method. IEEE Signal Process Lett. 23(5), 639–643 (2016)